ELSEVIER

Journal of Alloys and Compounds 320 (2001) 133–139

Journal of ALLOYS AND COMPOUNDS

www.elsevier.com/locate/jallcom

Hydrogen storage properties of the mechanically alloyed $LaNi_5$-based materials

G. Liang*, J. Huot, R. Schulz

Hydro-Quebec Research Institute, 1790 Boul. Lionel-Boulet, Varennes, QC, Canada J3X 1S1

Received 8 January 2001; accepted 19 January 2001

Abstract

Mechanical alloying has been used to synthesize $LaNi_5$-based hydrogen storage alloys. Mechanical milling of the La and Ni powder blend results in the direct formation of nanocrystalline AB_5 phase. Hydrogen storage measurements show that this as-milled $LaNi_5$ compound does not absorb much hydrogen reversibly. Annealing leads to grain growth, release of microstrain, and to an increase of storage capacity. Substitution of La or Ni by a third element can easily be achieved by mechanical alloying. The structure and hydrogen storage properties of these $LaNi_5$-based alloys prepared by mechanical alloying and annealing show no big difference with those of melt casting alloys.

Keywords: Hydrogen absorbing materials; Rare earth compounds; Nanostructured materials; Mechanical alloying

1. Introduction

$LaNi_5$- and $MmNi_5$-based alloys have been widely investigated as hydrogen storage materials [1,2]. These alloys are commonly prepared by conventional melt casting method. Cast alloys are usually melted several times, and the produced ingots are often annealed at high temperatures (above 1000°C) for long times, in order to get rid of any compositional segregation. After such treatment, the ingot has to be pulverized by mechanical grinding or hydrogenation before use [3,4].

Recently, mechanical alloying and mechanical grinding have been used to synthesize or treat AB, AB_5, AB_2 and Mg-based hydrogen storage materials, and a good improvement in activation and kinetics has been achieved [5–16]. However, a severe loss of hydrogen storage capacity was observed in the AB, AB_5 and AB_2 systems [5–14], but not much in the Mg_2Ni and Mg systems [15,16]. The loss of storage capacity was explained by the formation of amorphous or disordered structures [5,8,12,13], or by the introduction of oxygen or nitrogen during milling [6,10,11]. An opposite result was claimed in a US patent [17], in which nanostructured AB_5 and AB_2 alloys show higher storage capacity than large-grain alloys. Evidently, the reasons for the change in capacity have not been well understood. In this work, we report the mechanosynthesis and the hydrogen storage properties of the AB_5 type alloys.

2. Experimental

The mechanical alloying was performed under argon atmosphere using a Spex 8000 ball mill. La, LaH_3, Mm, Ni, Zn and Mg powders with purity better than 99.5% were used as raw materials. The Mm and La powders were prepared inside a glove-box by pulverizing the ingots. The mischmetal Mm contains 51%Ce, 26.4%La, 16.4%Nd and 5.3%Pr. The $LaNi_5$ powder used for mechanical milling was purchased from JMC. The powders in the desired composition were mixed and mechanically milled in a steel vial filled with three steel balls of diameter 11 cm. The ball to powders mass ratio was 10:1.

The post-milling isothermal annealing was done under a vacuum better than 10^{-4} Torr. The hydrogen storage properties were evaluated by using an automatic Sieverts apparatus. The X-ray powder diffraction was performed on

*Corresponding author. Tel.: +1-450-652-8106; fax: +1-450-652-8334.

E-mail address: liang.guoxian@ireq.ca (G. Liang).

0925-8388/01/$ – see front matter
PII: S0925-8388(01)00929-X

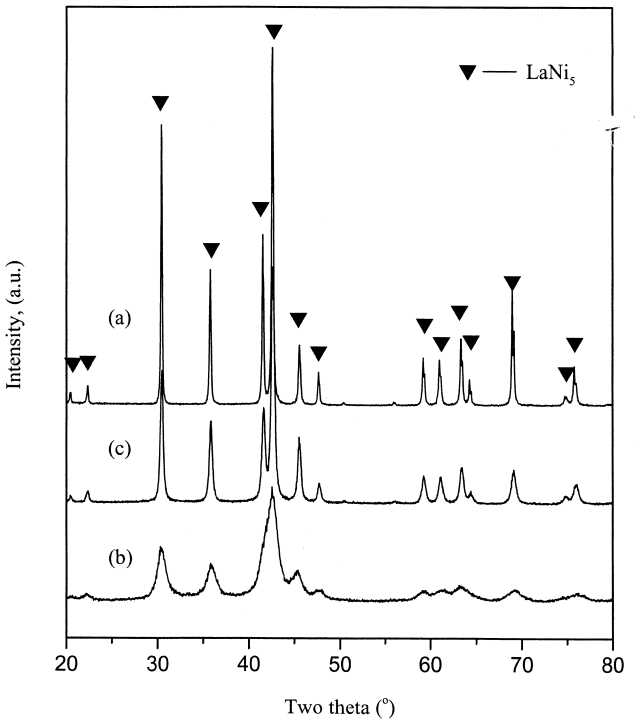

Fig. 1. XRD spectra of $LaNi_5$ (a) as-received, (b) as-milled and (c) after 3 h annealing at 550°C.

a Siemens D500 apparatus with Cu Kα radiation. The lattice parameters were determined from the diffraction peak positions. The crystallite size and microstrain were determined from peak broadening using the Williamson–Hall methods [18]. The peak position and peak broadening were calibrated by using strain free pure Si powders. The differential scanning calorimetry (DSC) measurement was performed on a Perkin-Elmer DSC7 apparatus with a scanning rate of 20°C/min. The powders were protected by N_2 flow during DSC measurement.

3. Results and discussion

3.1. Mechanical milling of the cast large-grain $LaNi_5$

The as-received cast $LaNi_5$ is single phase as determined by X-ray diffraction (XRD) shown in Fig. 1a. The sharp diffraction peaks in the X-ray spectrum indicate that the unmilled $LaNi_5$ has large crystallites. Mechanical milling of the cast $LaNi_5$ results in a substantial broadening of the X-ray diffraction peaks as shown in Fig. 1b, owing to the introduction of microstrain and reduction in grain size. Indeed, measurements show that the crystallite size and microstrain are 10.2±1.3 nm and 0.4%, respectively, after 5 h of mechanical milling. The lattice parameter of the $LaNi_5$ phase has been determined and is given in Table 1. We observed a decrease of the lattice parameter *a* and the unit cell volume and an increase of the lattice parameter *c*. This is probably related to the substitution of one lanthanum by a pair of nickel atoms (dumbbells) along the *c* axis. It was reported that the substitution of one lanthanum at the 1a site by a pair of Ni atoms induces shrinking of the unit cell along the *a* axis and cell volume, together with an expansion along the *c* axis [19,20].

Due to severe broadening, overlapping and reduction in intensities of diffraction peaks, it is very difficult to measure the lattice parameters of the as-milled nanocrystalline $LaNi_5$ with high precision. However, we do observe a trend that the lattice parameter *a* and the cell volume increase, while the lattice parameter *c* increases with increasing milling time. This is different from what was observed before for the ball-milled $LaNi_5$. Corre et al. [7] observed a slight increase of the lattice parameter *a* and the cell volume, while the *c* value remained basically unchanged when $LaNi_5$ was milled in a P-7 Fritsch planetary mill for up to 5 h. The milling intensity being lower in a P-7 than in a Spex mill, it is most likely not high enough to create site exchange between La and Ni, as we observed in our case using the Spex mill.

Table 1
Lattice parameters and hydrogen storage properties of various AB_5 alloys

Compounds	*a* (Å)	*c* (Å)	*V* (Å^3)	Capacity (wt.%)	Δ*H* (kJ/mol)	Δ*S* (J/mol K)
$LaNi_5$, cast alloy	5.0165	3.9794	86.7	1.40	−30[a]	−105[a]
$LaNi_5$, 5 h-milled	4.9991	3.9907	86.4	0.89		
$LaNi_5$, milled+annealing (550°C for 3 h)	5.0078	3.9818	86.5	1.38	–	–
$LaNi_5$, mechanical alloying +annealing	–	–	–	1.35	–	–
$LaNi_5$, prepared from LaH_3 and Ni	5.0019	3.9907	86.5	1.20	−28±0.6	−101.3±1.8
$LaNi_{4.9}Zn_{0.1}$	–	–	–	1.31	−31.5±0.5	−104.4±1.2
$LaNi_{4.7}Zn_{0.3}$	5.0207	3.9877	87.1	1.28	−32.8±0.3	−105.9±0.9
$LaNi_{4.7}Al_{0.3}$	5.0284	3.9964	87.5	1.22	−32.7±0.5	−105.5±1.6
$MmNi_{4.5}Al_{0.5}$	4.9543	4.0252	85.6	1.10	−28.4±0.4	−105.3±1.3
$La_{0.7}Ca_{0.2}Ce_{0.1}Ni_5$	4.9918	3.9801	85.9	1.29	−29.4±0.3	−106.6±0.8

[a] Values from Ref. [3].

The defects (dislocations, point defects) accumulated during mechanical grinding generally cause lattice expansion. It has been observed that the reduction in grain size to the nanometer range causes lattice distortion and an increase of unit cell volume [21]. However, we do not see unit cell expansion here. The effect of lattice expansion by strain and grain size reduction may be buried by the substitution effect which causes large unit cell shrinkage.

Isothermal annealing at 550°C for 3 h results in a substantial grain growth and an almost complete release of the microstrain. The average crystallite size is 28±2 nm, and the microstrain is 0.05% after annealing. We also observe that the lattice parameter *a* and the cell volume increase and the lattice parameter *c* decreases slightly after annealing in comparison to those of the as-milled powder (see Table 1). The lattice parameters of the 550°C-treated sample are close to those of the unmilled $LaNi_5$. This experiment clearly indicates that atom rearrangement (re-ordering) can be achieved by annealing at moderate temperatures. This can also explain why no significant change in lattice parameter and cell volume was observed in the high temperature annealed sample (>800°C) [6,9,10].

Fig. 2 shows the PCI curves of the $LaNi_5$ powders after different treatments. The unmilled $LaNi_5$ exhibits a flat plateau. The absorption/desorption plateau pressures are the same as those reported for $LaNi_5$ in the literature [22]. For the as-milled nanocrystalline powders, very sloping plateaus are observed for both absorption and desorption. The α phase region is extended and the overall storage capacity is reduced significantly. This is similar to what was observed in other nanocrystalline materials [12,13].

As stated in the above structural analysis, the grain size of $LaNi_5$ is diminished to 10 nm by mechanical grinding. If the thickness of the grain boundary is 1 nm, about 30% of the atoms are located in grain boundaries. Up to now, there has been little research on the hydrogen storage properties of grain boundaries in nanocrystalline materials. It was hypothesized that the grain boundary regions in some nanocrystalline materials are amorphous like and, therefore, their hydrogen storage properties should be similar to those of amorphous alloys [12,13]. This could partly explain the sloping plateaus and the loss of capacity.

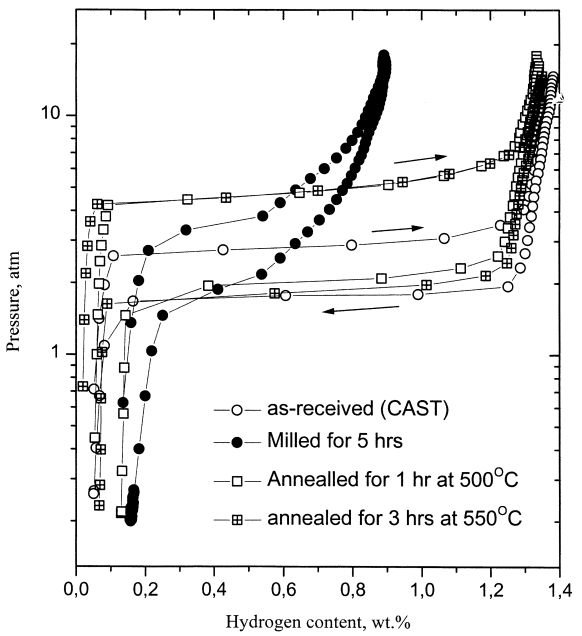

Fig. 2. PCI curves of the $LaNi_5$ alloys after different treatments.

Studies have shown that all the structurally isomorphic and chemically random $A_{1-x}B_x$ glasses (where A(B) is a late(early) transition metal) store hydrogen in their tetrahedral interstitial sites [23]. The maximum absorbed hydrogen-to-metal atomic ratio is related to these sites. The random local arrangement of atoms in the amorphous structure provides a wide distribution of energy of sites, and these energies depend on the A and B atoms. The general behavior is that the amount of hydrogen absorbed is reduced in comparison to that of the ordered structure under the same conditions, and that there is no plateau region in the PCI curves. If the grain boundary region of the as-milled $LaNi_5$ is amorphous like, the storage capacity in the grain boundary region is less than 0.2H/M [23], i.e. only 1/5 of that of the crystalline $LaNi_5$. Therefore, the total capacity of the nanocrystalline as-milled $LaNi_5$ is only 76% of that of the large-grain unmilled AB_5 compound. In fact, our measurements show that the storage capacity of the as-milled (5 h) $LaNi_5$ is only 64% of the unmilled one. Therefore, there must be other factors causing additional reductions of the storage capacity.

Tessier and co-workers [12,13] proposed that the nanostructured FeTi can be considered as a composite of crystalline nano-grains and highly disordered (amorphous-like) grain boundary regions. They argued that the narrowing of the miscibility gap for nano-FeTi is largely due to the presence of an amorphous component reducing the amount of material involved in the α–β transformation. An additional reduction caused by the elastic stress between the nanograins and the amorphous grain boundaries was proposed [12]. There is no doubt that the local stress and strain have great effects on the occupation of hydrogen atoms in the interstitial sites.

As pointed out previously, another change in structure is the lattice distortion, which is reflected in the microstrain. Recent investigations [24–26] indicate that microstrain especially the anisotropic one induced by the hydriding–dehydriding reaction is responsible for the loss of capacity of the AB_5 alloys upon long-term cycling. The large microstrain in the as-milled $LaNi_5$ is most likely one factor responsible for the observed reduction of the hydrogen storage capacity.

The chemical disorder or site exchange of La and Ni atoms will undoubtedly cause a change in the number of storage sites and their energies. We may expect formation of some stable sites which remain occupied under dehydriding conditions causing an overall lower reversible

storage capacity. It was also hypothesized that some 3f and 6m sites for hydrogen atoms around the dumbbell atoms are blocked by the coulombic potential barrier of the latter, when La atoms are replaced by Ni dumbbells. This also caused a decrease in the hydrogen storage capacity [27].

Isothermal annealing leads to a gradual recovery of the storage capacity. The desorption plateau pressure decreases with increasing annealing temperature. The plateau becomes fairly flat after 1 h annealing at 500°C (Fig. 2). After 3 h annealing at 550°C, the full storage capacity has almost been recovered. The desorption plateau pressure is close to that of the unmilled alloy. The absorption plateau is much higher, and the hysteresis is bigger. After five absorption/desorption cycles, no decrease in hysteresis is observed. This is different from what was reported by Luo et al. [28] and by Goodell [29]. This behavior is not well understood yet. Notten et al. [19] proposed that the dumbbell pairs, replacing the La atoms within the AB_5 structure, have a smaller hydrogen affinity. Consequently, the free energy of the formation of the hydride is less negative which implies higher plateau pressures. Nevertheless, more work is needed to get a better understanding of this phenomenon.

3.2. Mechanical alloying of the La+5Ni powder blend

Fig. 3 shows the XRD spectra of the La+5Ni powder blend mechanically alloyed for various times. After 1 h of milling, the diffraction peaks of Ni are very strong; however, those of La can barely be seen. After 5 h of milling, the $LaNi_5$ phase forms and only small Ni peaks can be observed. Increasing milling time to 40 h does not lead to further change. The mechanically alloyed $LaNi_5$ shows a nanocrystalline AB_5 structure. Again, heat treatment at elevated temperatures gives rise to grain growth and a full incorporation of Ni into the AB_5 lattice.

As observed in the mechanically milled $LaNi_5$, a sloping PCI curve is also obtained in the case of the mechanically alloyed nanocrystalline powders. The hydrogen storage capacity increases with increasing annealing temperatures. However, the desorption plateau pressures decrease and the hysteresis increases at the same time, as shown in Fig. 4. In comparison to that of the mechanically ground $LaNi_5$, higher annealing temperatures (100°C higher) are needed to achieve similar structure and hydrogen storage properties. This means that the local arrangement of the mechanically alloyed and mechanically milled nanocrystalline $LaNi_5$ are slightly different. For the mechanically alloyed one, more structural and chemical rearrangement is needed to restore full storage capacity.

3.3. Synthesis of $LaNi_5$ by ball milling LaH_3+5Ni followed by a heat treatment

The XRD spectra of LaH_3+5Ni milled for various times are shown in Fig. 5. The Ni peaks are still present after 20 h of milling. The peak position of Ni does not change. The peak intensity of LaH_3 is decreasing rapidly with increasing milling time. After 5 h of milling, small peaks of the α-$LaNi_5H_{0.15}$ phase appeared. However, increasing milling time to 20 h does not lead to a transformation of LaH_3+5Ni to $LaNi_5$ or β-hydride.

DSC measurements show that the mechanically milled powder mixture undergoes a structural transformation upon heating (Fig. 5). The reaction of formation of the $LaNi_5$ phase takes place at a temperature higher than 300°C. The low temperature shoulder with an onset at 155°C (see

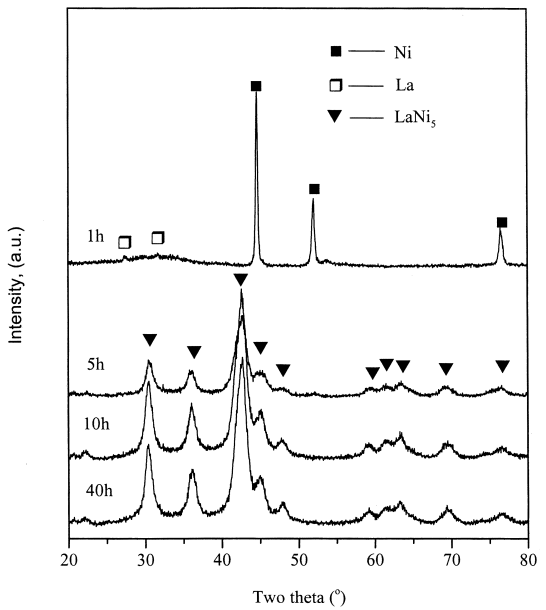

Fig. 3. XRD spectra of the La+Ni powder blend mechanically alloyed for various times.

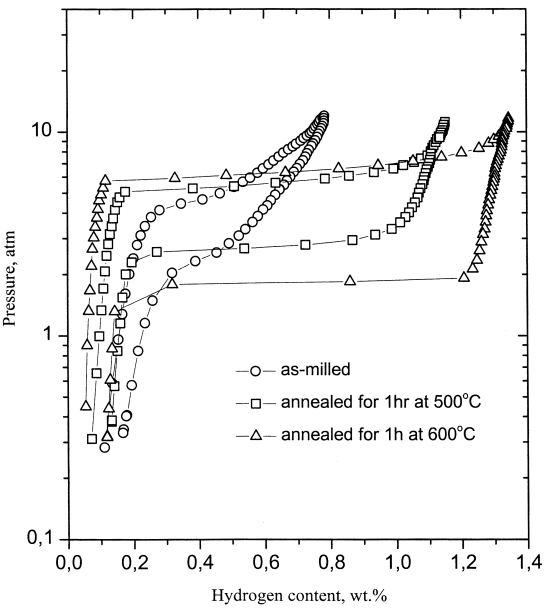

Fig. 4. PCI curves of the mechanically alloyed $LaNi_5$.

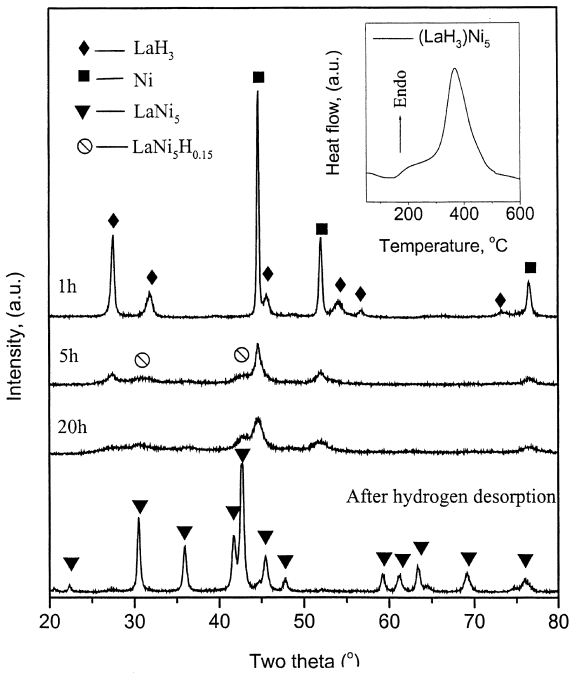

Fig. 5. XRD spectra of the LaH_3+5Ni powder blend milled for various times, and the insert DSC trace of the $(LaH_3)Ni_5$ milled for 40 h.

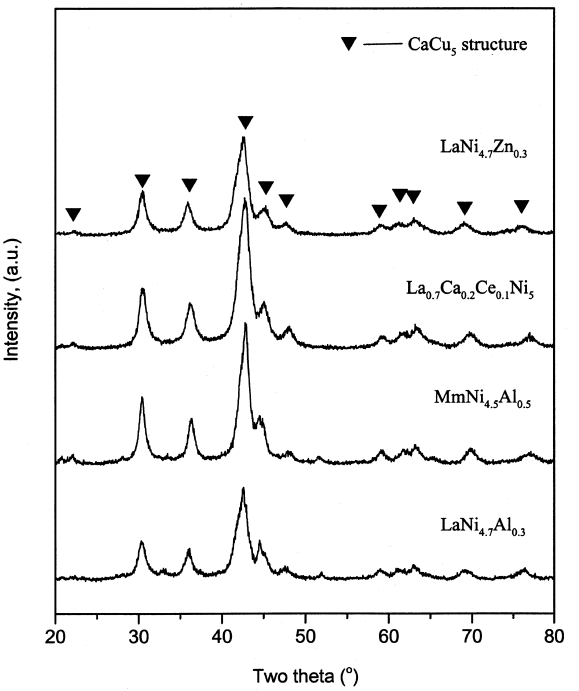

Fig. 6. XRD spectra of various mechanically alloyed alloys.

insert of Fig. 5) is probably related to the hydrogen desorption from the α phase.

The hydrogen storage properties of the $LaNi_5$ alloy obtained by mechanical milling of the LaH_3+5Ni mixture followed by annealing are similar to those of the mechanically alloyed $LaNi_5$, except that the storage capacity is slightly smaller and the plateau pressure is higher after the same annealing treatment. The lattice parameters and the unit cell volume of the $LaNi_5$ prepared by this method are also shown in Table 1. The lattice parameter *a* and cell volume are smaller than those of unmilled or stoichiometric $LaNi_5$ alloy. As reported before, the lattice parameter *a* decreases and *c* increases with increasing Ni content for over-stoichiometric alloys [30]. According to this report, the values of the present alloy would correspond to $LaNi_{5.2}$. This could explain the higher plateau pressure and the reduced storage capacity of the present alloy [30]. In the X-ray spectrum, there are still small peaks of LaH_3 left even after 2 h exposure to high vacuum. This is also consistent with the fact that the $LaNi_5$ compound synthesized this way is Ni rich.

3.4. Addition of third elements by mechanical alloying

Fig. 6 shows the XRD spectra of various alloys prepared by mechanical alloying. Owing to the broadening and overlapping of diffraction peaks, it is difficult to say whether all elements go into solid solution. Annealing at 600°C for 2 h leads to grain growth as before (see Fig. 7). In the cases of $LaNi_{4.7}Zn_{0.3}$, $LaNi_{4.7}Al_{0.3}$ and $La_{0.7}Ca_{0.2}Ce_{0.1}Ni_5$, a small Ni peak is present in addition to the AB_5 phase. In the case of $MmNi_{4.5}Al_{0.5}$, small peaks of NiAl phase appeared.

The lattice parameters of various substituted alloys are given in Table 1. The Zn and Al substitutions for Ni lead to lattice expansion of the $LaNi_5$ phase. The measured lattice parameters and the unit cell volume of the me-

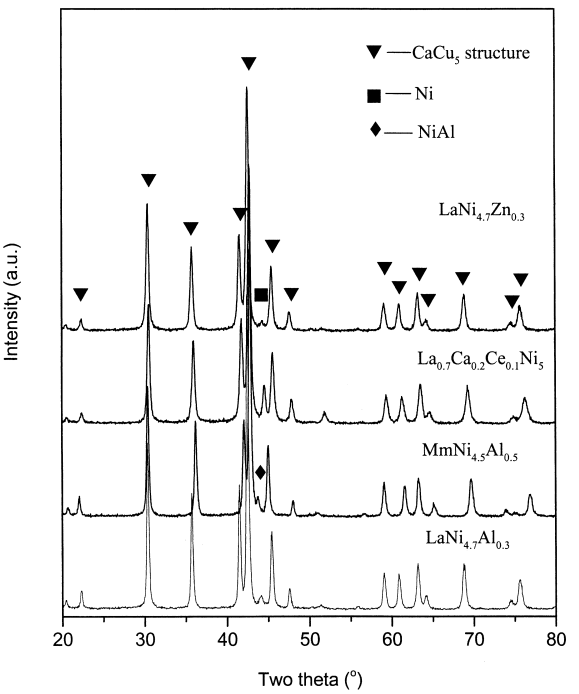

Fig. 7. XRD spectra of various alloys after 2 h annealing at 600°C.

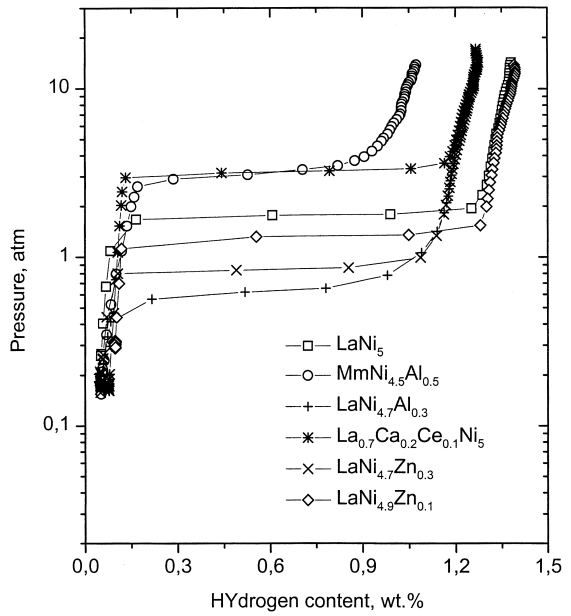

Fig. 8. Representative desorption PCI curves of various mechanically alloyed alloys.

chanically alloyed alloys are the same as those reported in the literature [31,32].

Fig. 8 shows a set of desorption PCI curves of the alloys prepared by mechanical alloying and annealing. It can be seen that the plateau pressure is reduced by replacing Ni by Zn and Al. The reaction enthalpy and entropy have also been determined by Van't Hoff methods and are given in Table 1. In comparison with those reported previously in the literature, we conclude that the mechanical alloying followed by low temperature annealing can produce similar alloys as those obtained by conventional induction or arc melting methods.

4. Conclusions

From our study of the mechanically alloyed $LaNi_5$-based materials, the following conclusions can be drawn.

1. Mechanical milling of cast $LaNi_5$ leads to a reduction of the grain size to the nanometer range and introduces disorder into the structure. The storage capacity is reduced in parallel. Annealing leads to reordering and recovery of the storage capacity.
2. Mechanical alloying of La and Ni powder blends leads to the direct formation of the nanocrystalline $LaNi_5$ phase. This mechanically alloyed $LaNi_5$ shows a behavior similar to that of mechanically milled $LaNi_5$.
3. Mechanical milling of LaH_3 with Ni leads to the formation of the α-$LaNi_5$ hydride phase. After 40 h of milling, a mixture of α-hydride phase+Ni+LaH_3 is obtained. An annealing at 500°C in vacuum gives rise to the formation of $LaNi_5$ phase, which exhibits similar hydrogen storage properties to those of mechanically alloyed $LaNi_5$.
4. Replacement of La by Ca, Ce, Mm, and Ni by Zn, Al can be achieved by mechanical alloying. After isothermal annealing, the structure of the $LaNi_5$ type alloys and their hydrogen storage properties are comparable to those produced by induction or arc melting.

Acknowledgements

The authors would like to thank M. Latroche of CRNS for helpful comments.

References

[1] K.H.J. Buschow, in: K.A. Gschneidner Jr., L. Eyring (Eds.), Handbook on the Physics and Chemistry of Rare Earths, Vol. 6, Elsevier, Amsterdam, 1984, Chapter 47.
[2] T. Sakai, in: K.A. Gschneidner Jr., L. Eyring (Eds.), Handbook on the Physics and Chemistry of Rare Earths, Vol. 21, Elsevier, Amsterdam, 1995, Chapter 142.
[3] G. Sandrock, State-of-the-art review of hydrogen storage in reversible metal hydrides for military fuel cell applications, ADA328073, 1997.
[4] T. Sakai, H. Yoshinaga, H. Miyamura, N. Kuriyama, H. Ishikawa, J. Alloys Comp. 180 (1992) 37.
[5] B.H. Liu, Z.P. Li, C.P. Chen, W.H. Liu, Q.D. Wang, J. Alloys Comp. 231 (1995) 820.
[6] C. Lenain, L. Aymard, F. Salver-Disma, J.B. Leriche, Y. Chabre, J.M. Tarascon, Solid State Ionics 104 (1997) 237.
[7] S. Corre, M. Bououdina, N. Kuriyama, D. Fruchart, G.Y. Adachi, J. Alloys Comp. 292 (1999) 166.
[8] A. Anani, A. Visintin, K. Petrov, S. Srinivasan, J.J. Reilly, J.R. Johnson, R.B. Schwarz, P.B. Desch, J. Power Sources 47 (1994) 261.
[9] M.L. Wasz, P.B. Desch, R.B. Schwarz, Phil. Mag. A 74 (1996) 15.
[10] M.L. Wasz, R.B. Schwarz, Mater. Sci. Forum 225–227 (1996) 859.
[11] L. Aymard, C. Lenain, L. Courvoisier, F. Salver-Disma, J.M. Tarascon, J. Electrochem. Soc. 146 (1999) 2015.
[12] P. Tessier, R. Schulz, J.O. Strom-Olsen, J. Mater. Res. 13 (1998) 1538.
[13] L. Zaluski, A. Zaluska, P. Tessier, J.O. Strom-Olsen, R. Schulz, J. Alloys Comp. 227 (1995) 53.
[14] M. Jurczyk, W. Rajewski, G. Wojcik, W. Majchrzycki, J. Alloys Comp. 285 (1999) 250.
[15] L. Zaluski, A. Zaluski, J.O. Strom-Olsen, J. Alloys Comp. 217 (1995) 245.
[16] J. Huot, G. Liang, S. Boily, A. Van Neste, R. Schulz, J. Alloys Comp. 293–295 (1999) 495.
[17] S.R. Ovshinsky, M.A. Fetcenko, J.S. Im, K. Young, B.S. Chao, B. Reichman, US patent 5840440.
[18] H.P. Klug, L. Alexander, in: X-Ray Diffraction Procedures for Polycrystalline and Amorphous Materials, 2nd Edition, Wiley, New York, 1974.
[19] P.H.L. Notten, R.E.F. Einerhand, J.L.C. Daams, Z. Phys. Chem. Bd. 183 (1994) 267.
[20] T. Vogt, J.J. Reilly, J.R. Johnson, G.D. Adzic, J. McBreen, Electrochem. Solid State Lett. 2 (1999) 111.
[21] Y.H. Zhao, K. Zhang, K. Lu, Phys. Rev. B 56 (1997) 14322.
[22] L.J. Swartzendruber, G.C. Carter, D.J. Kahan, M.E. Read, J.R. Manning, in: T.N. Veziroglu, W. Seifritz (Eds.), Proc. 2nd World

Hydrogen Energy Conference, Zurich, Switzerland, Hydrogen Energy System, 1978, p. 1973.
[23] J.H. Harris, W.A. Curtin, M.A. Tenhover, Phys. Rev. B 36 (1987) 5784.
[24] Y. Nakamura, K. Sato, S. Fujitani, K. Nishio, K. Oguro, I. Uehara, J. Alloys Comp. 267 (1998) 205.
[25] H. Nakamura, K. Oguro, I. Uehara, E. Akiba, Int. J. Hydrogen Energy 25 (2000) 531.
[26] M.P. Pitt, E.MacA. Gray, E.H. Kisi, B.A. Hunter, J. Alloys Comp. 293–295 (1999) 118.
[27] K. Yasuda, J. Alloys Comp. 253–254 (1997) 621.
[28] S. Luo, J.D. Clewley, T.D. Flanagan, R.C. Bowman Jr., L.A. Wade, J. Alloys Comp. 267 (1998) 171.
[29] P.D. Goodell, J. Less-Common Met. 99 (1984) 1.
[30] K.H.J. Buschow, H.H. Van Mal, J. Less-Common Met. 29 (1972) 203.
[31] B. Rozdzynska-kielbik, W. Iwasieczko, H. Drulis, V.V. Pavlyuk, H. Bala, J. Alloys Comp. 298 (2000) 237.
[32] T. Kodama, J. Alloys Comp. 289 (1999) 207.